applied sciences

MDPI

Article

Optimizing Retention Bunkers in Copper Mines with Numerical Methods and Gradient Descent

Piotr Bortnowski [1,*], Robert Król [1], Natalia Suchorab-Matuszewska [1], Maksymilian Ozdoba [1] and Mateusz Szczerbakowicz [1,2]

[1] Department of Mining, Faculty of Geoengineering, Mining and Geology, Wroclaw University of Science and Technology, ul. Na Grobli 15, 50-421 Wroclaw, Poland; robert.krol@pwr.edu.pl (R.K.); natalia.suchorab@pwr.edu.pl (N.S.-M.); maksymilian.ozdoba@pwr.edu.pl (M.O.); mateusz.szczerbakowicz@pwr.edu.pl (M.S.)

[2] KGHM Polska Miedź S.A., Rudna Mine, ul. Henryka Dąbrowskiego 50, 59-100 Polkowice, Poland

* Correspondence: piotr.bortnowski@pwr.edu.pl

Abstract: This study examines the optimization of ore receiving bins in underground copper mines, targeting the reduction of rapid wear and tear on bin components. The investigation identifies the primary wear contributors as the force exerted by the accumulated ore and the velocity at which ore particles move. By altering design and operational parameters, the objective is to decrease wear at key points such as transfer areas, thereby improving the efficiency and service life of retention bunkers. A Discrete Element Method (DEM) model of the bin was created and validated against actual mining conditions to study the impact of material flow on wear. The optimization approach used a constrained gradient descent algorithm to minimize factors like particle velocity and pressure force, while maintaining the efficiency of the bin. The findings provide valuable insights for the future design enhancements, potentially improving the operational performance of retention bunkers in the mining industry.

Keywords: retention bunker; discrete element method; wear damage; failure analysis; reliability optimization

check for updates

Citation: Bortnowski, P.; Król, R.; Suchorab-Matuszewska, N.; Ozdoba, M.; Szczerbakowicz, M. Optimizing Retention Bunkers in Copper Mines with Numerical Methods and Gradient Descent. *Appl. Sci.* **2024**, *14*, 2612. https://doi.org/10.3390/app14062612

Academic Editor: Nikolaos Koukouzas

Received: 18 February 2024
Revised: 15 March 2024
Accepted: 16 March 2024
Published: 20 March 2024

Copyright: © 2024 by the authors. Licensee MDPI, Basel, Switzerland. This article is an open access article distributed under the terms and conditions of the Creative Commons Attribution (CC BY) license (https://creativecommons.org/licenses/by/4.0/).

1. Introduction

The transportation system plays a important role in the entire mining process [1]. Due to the specific method of exploitation using a room-and-pillar system, the transportation system in underground copper ore mines is highly complex [2]. Owing to the widespread use of conveyor belts in material transport [3], there are many strategic points along the route where the ore is transferred from one conveyor to another [4]. This is necessary due to changes in the direction of transport or differences in the elevations of the conveyor belts. Some of the most important elements in the considered transportation system are retention bunkers, which are recognized as a specific, large structure, practically encountered only in this type of mining [5]. Their main task is to maintain the continuity of ore flow, minimize fluctuations associated with changes in material flow, and accumulate the ore [6]. The design of such devices has a significant impact on their operational parameters and should ensure effective, reliable, and safe operation [7]. However, due to the scale and the amount of the material flowing through them [8], they are exposed to various risks. Therefore, a very important aspect is understanding the loads acting on the receiving bin structure located under the retention bunker, which is directly subjected to all static forces from the vertical column of material and dynamic forces from falling rocks [9]. At the loading points of transfer chutes, or retention bunkers, the ore falls onto steel elements and the conveyor belt with a certain force whose value depends on its size and velocity, as well as the geometry of the structure [10]. The geometry of the elements on which the ore impacts

and slides affects their durability, and causes the loss of physical properties [11]. Moreover, it can cause blockages and limit the transport capabilities of the entire ore handling system.

Due to the specificity of retention bunkers, the number of research studies in this area is very limited, especially when it comes to similar structural solutions, with a primary focus on ore receiving bins. Current research primarily concentrates on the design and structural strength analysis of retention bunkers, considering the loads imposed by the surrounding rock mass [12]. However, these studies are less focused on analyzing structural damage or wear of steel surfaces in retention bunker elements resulting from contact with ore. One of the key challenges in designing such equipment is the gap in knowledge regarding the magnitude and distribution of forces exerted by the ore mass on the structural components of the equipment, along with a shortage of established tools to determine these forces. Additionally, the impact of the design and operational factors of bins on the stress distribution on its structure and the impact on the degradation process have never been clearly formulated. The main factor influencing the process of accelerated abrasive wear is certainly the difference between the hardness of the chute elements and the transported material [13]. Vibrations in structures can significantly impact wear, as induced oscillations can lead to increased friction between moving parts, accelerating their degradation [14]. Additionally, uneven distributions of vibrations can cause uneven loads on structural elements, resulting in locally intensified wear, highlighting the necessity of precise modal analysis in the design and maintenance process [15].

In some optimization works related to conveyor transfer points, the use of numerical methods to simulate the behavior of flowing ore particles or other transported materials is a common practice [16]. Numerical methods are also used to optimize material flow on the conveyor itself or within it [17]. Typically, 3D DEM models are created to examine the wear of conveyor components during material transport, and their usefulness has been unequivocally confirmed [18–20]. They enable modeling of the particle flow, predicting stresses on elements interacting with particles, determining the degree of energy dispersion, and describing the segregation process [21]. The latter process, especially, is extensively analyzed due to various material flow variants in chutes [22,23]. In this research work [24], it was shown that the conveyor element and chute are more susceptible to wear with larger particle sizes, and the wear of the receiving belt is accelerated with a decrease in its speed. Previous research results show that the wear, stress, and accumulated contact energy of the transfer point chute are closely related to the belt speed, the angle of the chute's inclination, and the type of granular materials [25]. In other studies [26], it has been proven that the angle of inclination and the height of the transfer point in the transfer chute directly affect the speed and trajectory of the falling material, which in turn has a significant impact on the wear of both the chute and the conveyor belt. The geometry and type of deflector, as well as the number of shelves in the chute, determine the direction of material flow and its speed, which directly affects wear patterns and material transfer efficiency. Additionally, the physical properties of the transported material, such as the shape and size of particles, influence local changes in flow and material speed, which also significantly affects the wear of the chute and conveyor belt. Appropriate manipulation of parameter ranges in numerical modeling also allows minimizing fluctuations in power consumption of devices and ensuring adequate system throughput [27].

A detailed qualitative and quantitative analysis of operational issues with the receiving bin is presented in the paper [5]. The most frequent type of damage was abrasive wear of the top layer of steel elements in contact with the flowing material. Elements such as the vertical seals, the lining of the bin drawer, and the lining of the front wall of the receiving bin were most susceptible to abrasive wear.

Different algorithms are used to optimize the operating parameters of transfer points. In the work [28], the authors utilized the E-SVR Surrogate Model for results obtained through numerical simulation in the EDEM environment. The sole aim of the research was to minimize the maximum forces during the impact of falling material on the belt. In another study [29], the authors used raw results of numerical simulations to optimize the

design parameters of a scraper conveyor, based mainly on the obtained correlations. It is also possible to forecast wear and the impact of external factors on wear using regression methods, as was performed in a study [30] where the Plackett–Burman method was utilized. It is also common practice to rely on appropriate wear models [31], where results from numerical simulations or evolutionary models based on purely theoretical assumptions are used. The main issue with most conducted research is that the analysis is performed within a very narrow range of variability in design or operational parameters, and methods based on optimization through simple correlation analysis do not always provide clear results.

Considering all the presented research results, a clear conclusion can be formulated that for the design of transfer points, including those related to retention bunker receiving bins, the main factors influencing an accelerated degradation process are the force of the material pressing on the structural elements and the velocity of ore particle flow. The results of these studies unequivocally suggest that both changes in design and operational parameters may reduce wear in conveyor transfer point chutes and similar steel structures. Therefore, these assumptions can be implemented for the optimization of dosing devices. The main goal of this article is to limit the impact of ore mass on the device's structure and reduce the material flow speed to improve wear parameters while ensuring optimal performance of the receiving bin. This allows for the most efficient use of the operating point of the receiving bins. This article deals with the characteristics of retention bunkers and the problem of abrasive wear of bin elements. Key factors that could improve the efficiency of the receiving bins were identified, and an experiment was designed based on them, whose results were based on the material flow in a built 3D DEM model of the bin. The model was validated under real working conditions in an underground copper ore mine. The impact of all independent factors on the value of dependent factors in the experiment was determined. Optimization of the analyzed receiving bin's operation was conducted using a constrained gradient descent method [32], aiming to minimize the particle speed on the surface of the bin and the total force exerted on the bin, while maintaining required efficiency. The proposed optimization method allowed for considering the impact of all independent factors in the full possible design range, and in a clear, mathematically formalized way, determined the optimal operating point of the device. Thanks to the research results, guidelines for designing future retention bunker receiving bins were formulated. The innovation of the research results lay in the optimization of the bunker receiving bin's design using real structural loads, which had not been clearly defined until now. Based on simulation, it was proven that design changes to these unique structures allow for improvements in the bin's working conditions and potentially reduce damage.

2. Retention Bunker Design and Principles

This study analyzed field bunkers, which are characterized by different construction, location, and capacity compared to large-capacity shaft bunkers with a capacity of 6000 Mg (tonnes). The workspace is created using mining methods within the rock mass. The lower space is bounded by a steel structure, which serves as an artificial roof. Embedded within it are openings that guide the ore to bins, which are devices for delivering the ore to the receiving conveyor located in the sub-bunker section. In the over-bunker section, there is a dumping station for the ore conveyor, which is typically aligned with the bunker's axis. In cases where two feeding conveyors are installed, they are positioned to maximize the workspace and ensure smooth ore reception by the receiving bins. Installing the second conveyor in the sub-bunker section allows for the separation of the ore stream into independent directions, improves the efficiency of the bunker's operation, and allows for better utilization of its retention capacity. To ensure unobstructed ore flow, the bins must be spaced at a certain distance from each other, resulting in the creation of a dead space within the bunker that cannot be utilized.

At ore discharge points and near ore bunkers, ore receiving bins are used, the construction of which is shown in Figure 1. In this device, copper ore flows gravitationally from the bunker space to the bin, which narrows in the direction of material movement and is

bounded by four inclined walls. The surfaces of the receiving bin walls of the ore bin are lined with wear-resistant steel liners. In the bottom of the bin there is an outlet opening and drawer. This drawer is mounted on a carriage that performs reciprocating motion driven by a crank mechanism. The stroke of the drawer in each movement is approximately 10.5 cm. The bottom of the drawer, where the ore falls, is also lined with steel liners. The drawer is attached from below to rails supported on both sides by steel wheels typical of railway rolling stock. The drawer, along with the ore, moves relative to the walls of the receiving bin, which is why vertical seals are used. The role of the vertical seals is to prevent fine ore from getting outside the receiving bin. The extension of the receiving bin helps to stop the flow of ore when the device is not in operation.

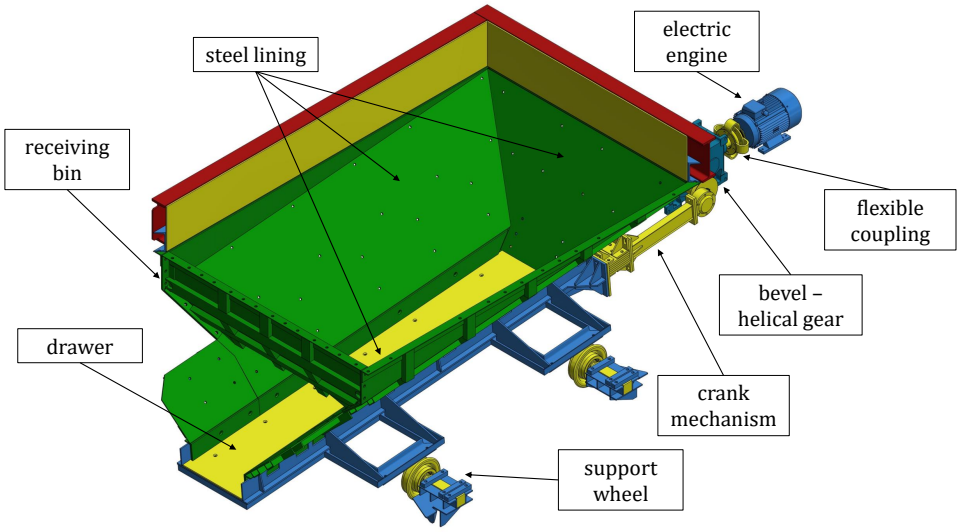


Figure 1. Construction of the ore receiving bin.

3. Materials and Methods

3.1. Experiment Design

Due to the substantial number of operations involved in the entire optimization process, the individual steps of the experiment have been illustrated using a flowchart. This chart is presented in Figure 2.

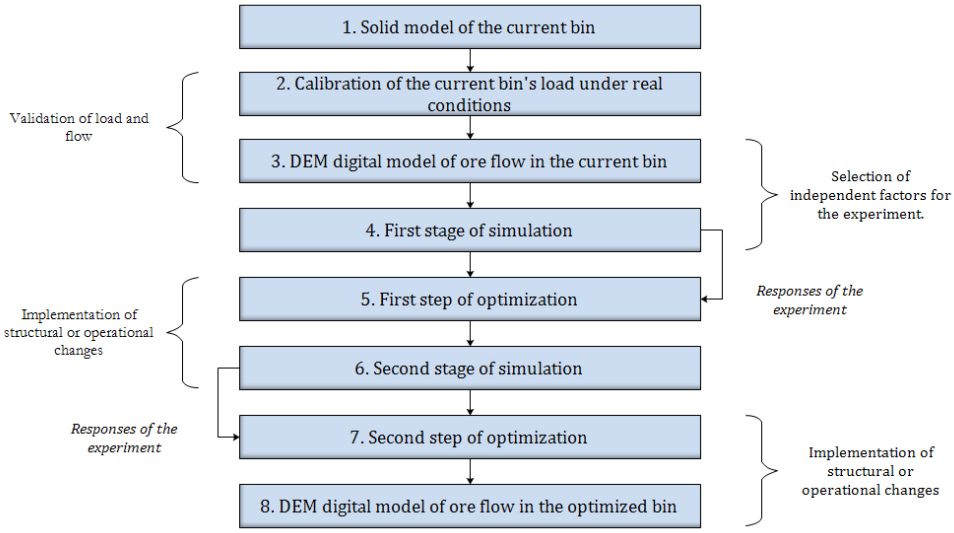


Figure 2. Flowchart illustrating the phases of the experiment in the optimization process.

Firstly, the optimization process began with the construction of a three-dimensional model of the receiving bin. For the purposes of modeling, one of the bins used in an underground copper ore mine was selected, and its detailed geometry was transferred to a computer environment. The modeled retention bunker (Figure 3a) has a maximum capacity of 2000 Mg and is integrated with a conveyor delivering ore (Figure 3b) and a conveyor responsible for receiving ore from the bin drawer (Figure 3c). The analyzed receiving bin is presented in Figure 3d.

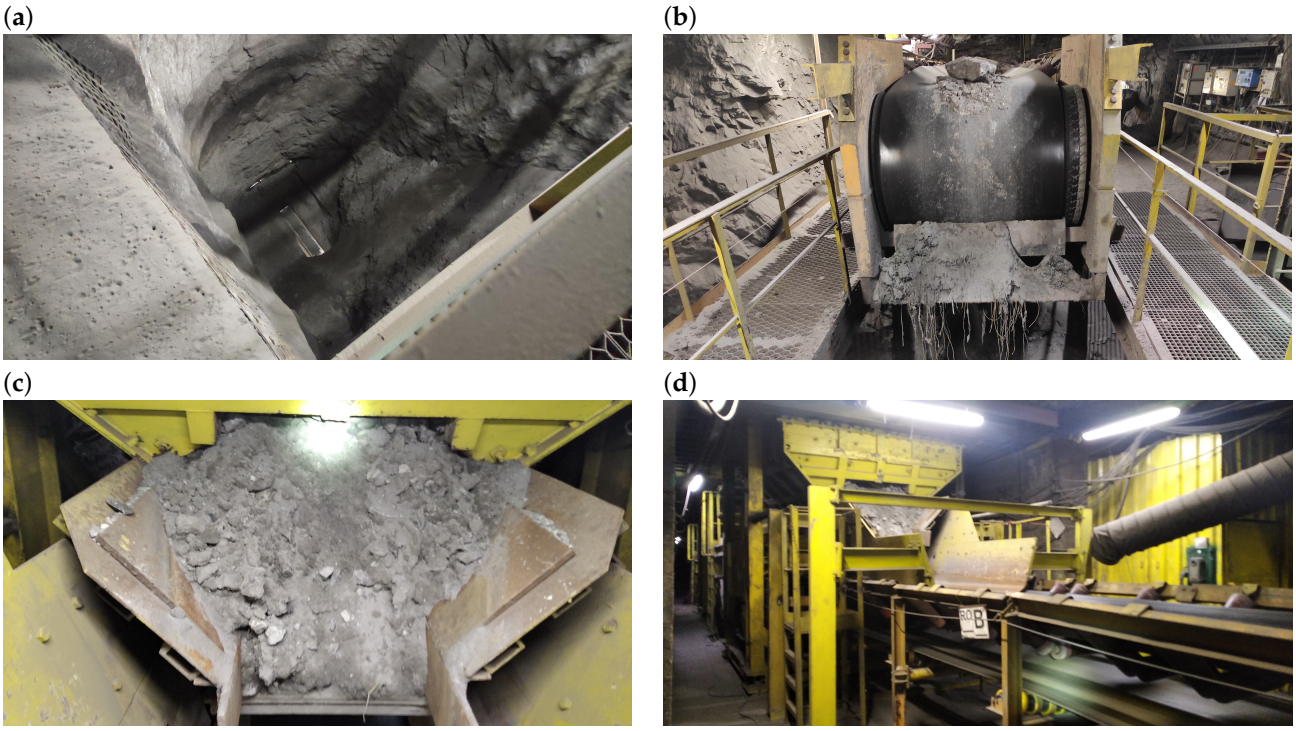


Figure 3. The retention bunker subjected to analysis includes: (**a**) the storage space of the retention bunker, (**b**) the feeding conveyor, (**c**) the receiving bin chute to the receiving conveyor, and (**d**) the structure of the receiving bin.

Secondly, in the optimization process, the characteristics of the bin drawer load under real working conditions were determined. This was performed by installing a measurement system that monitored the load on the support wheels during the normal cycle of filling the retention bunker and the flow of ore. These results enabled the validation of the digital model of ore flow, which was developed in the next step of the optimization process. For modeling the ore flow in the retention bunker, material and quality parameters of the copper ore and construction materials of the bin, determined under laboratory conditions, were used. The operating parameters of the devices were set in accordance with their real values. The conveyor belt speed was set at 2.5 m/s, and the frequency of the bin drawer movement was 1.38 Hz. The extension of the bin drawer, resulting from its geometry, reached 0.105 m. The modeled length of the bin drawer was 3.98 m, the area of the outlet opening was 0.72 m^2, and the angle of inclination of the drawer was 4.86°.

Based on the results of the ore flow simulation in the current bin design, independent factors were identified, which were subject to modification during the experiment. The numerical experiment was divided into two stages. In both stages of the simulation, the primary aim of optimization was set to minimize the force F pressing on the drawer of the bin and the average velocity v of particles on the drawer, while maintaining the current capacity Q. It was assumed that Q should not fall below 90% of its current value Q_c. These parameters were the dependent factors in the conducted experiment. Experiments for both stages of simulation and optimization were carried out using a factorial method, analyzing all possible combinations of independent factors. Table 1 presents the range of

parameter modifications for the two stages of modification. Figure 4 shows the location of independent factors in relation to the receiving bin's design.

Table 1. Levels of independent factors in the experiment.

Stage No.	Independent Factor	Unit	Value		
			Min	Mean	Max
1	L	m	2.98	3.48	3.98
1	d	m	0	0.5	1
2	f	Hz	0.63	1.1	1.57
2	S	m^2	0.64	1.005	1.37
2	β	°	4.86	6.86	8.86

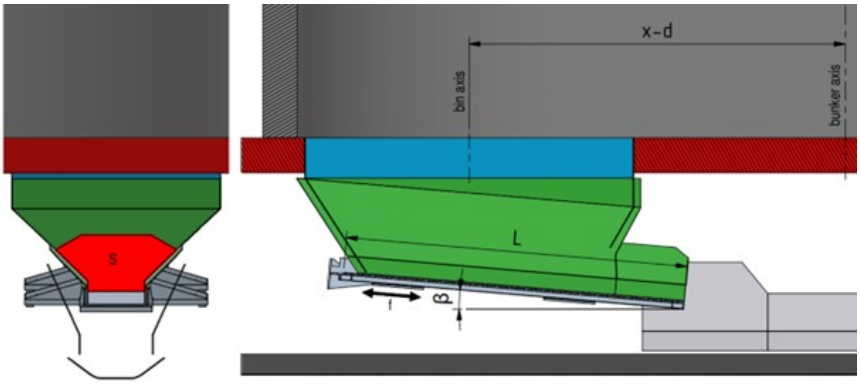


Figure 4. Independent factors in relation to the receiving bin's design.

In the first stage, to eliminate design flaws affecting uneven load distribution and insufficient use of the drawer's workspace, two independent factors were defined for evaluation. The first was the length of the drawer L, corresponding to the total length of the bin, while the second was the offset of the retention bunker axis d, aimed at ensuring an even distribution of load on the drawer's surface. These constraints included maintaining the existing geometry of the bunker and the required distance between the bins. The optimal variant was selected using a simple method of filtering responses (dependent factors) from various scenarios, and the identified modifications served as a starting point for the second stage of simulation and optimization. This approach to optimization was chosen due to the limited ability to adjust the selected parameters.

During the second stage of the simulation, three additional independent factors were evaluated. Based on operational experience and the complexity of further implementation, one operational factor was selected—the frequency of the drawer movement f—as well as two design factors: the surface area of the bin's outlet opening S and the angle of inclination of the drawer β. Adjusting the drawer movement frequency is an operational parameter that can be easily tailored to operational requirements, for example, by controlling the operation of the drive motor or changing the gear ratio of the drive transmission. The other two design factors are relatively easy to design and implement, both in existing and new containers. In the second stage, to determine the optimal design, a constrained gradient descent method was utilized. For the analysis, a linear dependence of dependent factors (responses) on independent factors was assumed.

Based on the results obtained in the two optimization stages, a digital simulation of the ore flow in the bin was carried out again, incorporating all the operational and design changes. The obtained results were compared with the values achieved in simulations of the currently used bin.

3.2. Calibration of the DEM Model

The measurement system was based on linear strain gauges (Figure 5). For each of the two examined supports, strain gauges were connected in a full bridge configuration to record the bending process of the wheel support axis under the weight of the excavated material. The measurement process captured the amplitude of the voltage signal from strain gauges, omitting the spectral processing usually employed in similar types of measurements [33,34]. For the purposes of the experiment, a symmetrical load distribution on the support wheels in the cross-section of the receiving bin was assumed. The measurement system was initially characterized under laboratory conditions, and then a proper calibration was conducted in underground conditions. During the research, the pressure force on the supporting wheels, the bin capacity using a conveyor belt measuring scale system, and the bunker filling level were measured.



Figure 5. Strain gauge full-bridge measurement system on the support wheel of the ore bin.

3.3. Ore Flow and Particle Contact Model

The Hertz–Mindlin (no slip) contact model [35] was employed to simulate interactions between particles where no slippage occurs [36]. A simplified diagram of the Hertz–Mindlin model is shown in Figure 6.

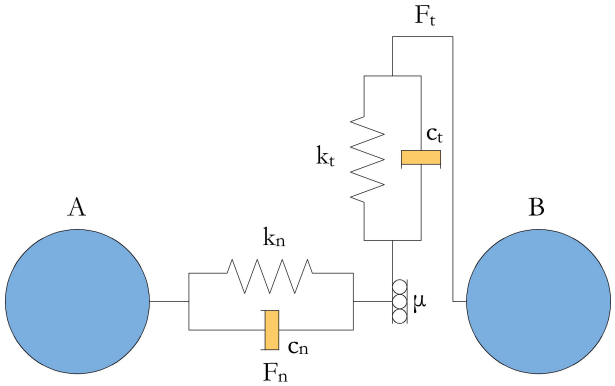


Figure 6. The simplified diagram of the Hertz–Mindlin model.

Within this model, the normal force F_n generated during contact is calculated using Hertz's contact theory, which is mathematically expressed as:

$$F_n = k_n \cdot \delta^n \tag{1}$$

where k_n is the normal stiffness constant, and δ^n is the normal deformation (compression) between particles.

The tangential force F_t, in accordance with the works of Mindlin and Deresiewicz [37,38], is determined based on plastic deformations at the contact and is expressed as:

$$F_t = k_t \cdot \delta^t \tag{2}$$

where k_t is the tangential stiffness constant, and δ^t is the tangential deformation.

Both forces include a damping component, proportional to the collision velocities of the particles and expressed as $-c_n \cdot v^n$ for the normal component and $-c_t \cdot v^t$ for the tangential component, where c_n and c_t are the damping coefficients, and v^n and v^t are the corresponding collision velocities.

Additionally, Coulomb's law is applied within this model to determine the maximum tangential friction force [39] $F_{t,\max}$, which is expressed as:

$$F_{t,\max} = \mu \cdot F_n \tag{3}$$

where μ is the coefficient of friction.

3.4. Material Parameters in the Model

The ore material for analysis was collected directly from conveyors transporting ore. The grain size curve was determined based on photographic documentation and validated with results from other studies conducted under similar conditions in the same copper ore mine [40]. After averaging the results, the D_{50}, which is the median particle size, is 9.43 mm, while the D_{80} is 109.95 mm. The other parameters of the ore were determined based on the method detailed in the paper [41] and are compiled in Table 2. The parameter values presented in the table are the final values of the model, which have been validated under laboratory conditions.

Table 2. Copper ore parameters adopted in the simulation.

Parameter	Unit	Value
Poisson's Ratio	-	0.24
Density	kg/m^3	2675
Young's Modulus	Pa	4.10×10^{10}
Angle of Natural Repose	°	35.37
Coefficient of Restitution	-	0.35
Coefficient of Static Friction	-	0.82
Coefficient of Rolling Friction	-	0.033

In the numerical model, ore particles interact with the steel and rubber elements of the receiving bin. Material parameters for steel and rubber were selected based on the results presented in the study [41], and then similarly calibrated under laboratory conditions. The material parameters adopted for steel and rubber are presented in Table 3.

Table 3. Steel and rubber parameters adopted in the simulation.

Parameter	Unit	Value	
		Steel	Rubber
Coefficient of Restitution	-	0.25	0.56
Coefficient of Static Friction	-	0.32	0.42
Coefficient of Rolling Friction	-	0.020	0.090

Based on the determined parameters of the materials in contact, the stiffness and damping coefficients in the model of moving particle contacts have been calculated.

3.5. Optimization Algorithm

In the first stage of optimization, an algorithm was applied that represents a simple optimization problem that can be formulated as follows:

$$\begin{aligned} &\text{Find } (L, d) \text{ such that:} \\ &\min_{L,d} F(L, d), \\ &\text{subject to} \\ &v(L, d) \text{ is minimized,} \\ &Q(L, d) \geq 0.9Q_c. \end{aligned} \tag{4}$$

In the second stage of optimization, the Constrained Gradient Descent Optimization algorithm was used. It is a mathematical optimization method employed to find the minimum or maximum of a function while taking specific constraints on variables into account. This method allows for the iterative adjustment of variables in the direction of the steepest descent, known as the negative gradient of the objective function, until a solution satisfying the specified constraints is reached. The general form of an optimization problem with constraints can be presented as follows, where the primary goal is to minimize or maximize the function $f(x)$, subject to:

$$\begin{aligned} &g_i(x) \leq 0 \text{ for } i = 1, 2, \ldots, m \\ &h_j(x) = 0 \text{ for } j = 1, 2, \ldots, p \end{aligned} \tag{5}$$

where x represents the vector of decision variables that need to be optimized, $g_i(x)$ are inequality constraints and m is the total number of such constraints, and $h_j(x)$ are equality constraints and p is the total number of such constraints.

The gradient descent optimization method begins with an initial approximation of the value of x and iteratively updates it using the following formula:

$$x_n = x_{n-1} - \beta \nabla f(x_{n-1}) \tag{6}$$

where x_n is the updated value of x, x_{n-1} is is the previous value of x, β is the step size or learning rate, which determines how large the steps are taken in the direction of the negative gradient, ∇ is the gradient of the objective function at the current point x_{n-1}.

In the analyzed case, the method was used to find the optimal values of independent factors (f, S, and β) that minimize the objective function. The objective function is the sum of two output variables (F and v) obtained from linear regression models, while satisfying specified constraints for the output variable of receiving bin capacity Q. The aim is to find the optimal values of these variables that minimize the objective function:

$$f(x) = f(F) + f(v) \tag{7}$$

where $f(F)$ is the predicted value of the total pressing force on the drawer based on the linear regression model, and $f(v)$ is the predicted value of the average particle velocity based on the linear regression model.

The constraint of the objective function based on linear regression $f(Q)$ can be presented in the following way:

$$w_C = f(Q) - 0.9Q_c \geq 0 \tag{8}$$

The independent factors were scaled before the optimization process to eliminate the impact of variability ranges on the final optimization outcome.

4. Results

4.1. Calibration of the DEM Model

In Figure 7, the results of the calibrating process of the receiving bin are presented. Figure 7a shows the total load on the front set of wheel supports, Figure 7b shows the load on the back set of wheel supports, and Figure 7c illustrates the cumulative load on all wheel supports, which is equivalent to the force of the material on the bin's drawer. Figure 7d presents the range of retention bunker filling for which the calibration process was carried out.

The results clearly indicate that the majority of the load is carried by the front part of the bin drawer. The average pressure force on the front support wheels was 363 kN, while on the back set, it was only 74 kN, which constitutes just over 20% of the load on the front part of the drawer. The average total load on the bin's drawer was 438 kN, and its decrease during the emptying of the retention bunker from a filling level of 900 Mg to 550 Mg is practically imperceptible. The large fluctuations in the load on the back set of supports result from the construction's characteristics, which are irregularly loaded and undergo cyclic shocks in the vertical direction, leading to significant impact loads and accelerated wear. The load from the weight of the drawer of the bin alone on the support wheels without the filling of the retention bunker amounted to just over 14 kN, which is in line with the technical data and confirms the correctness of the calibration performed.

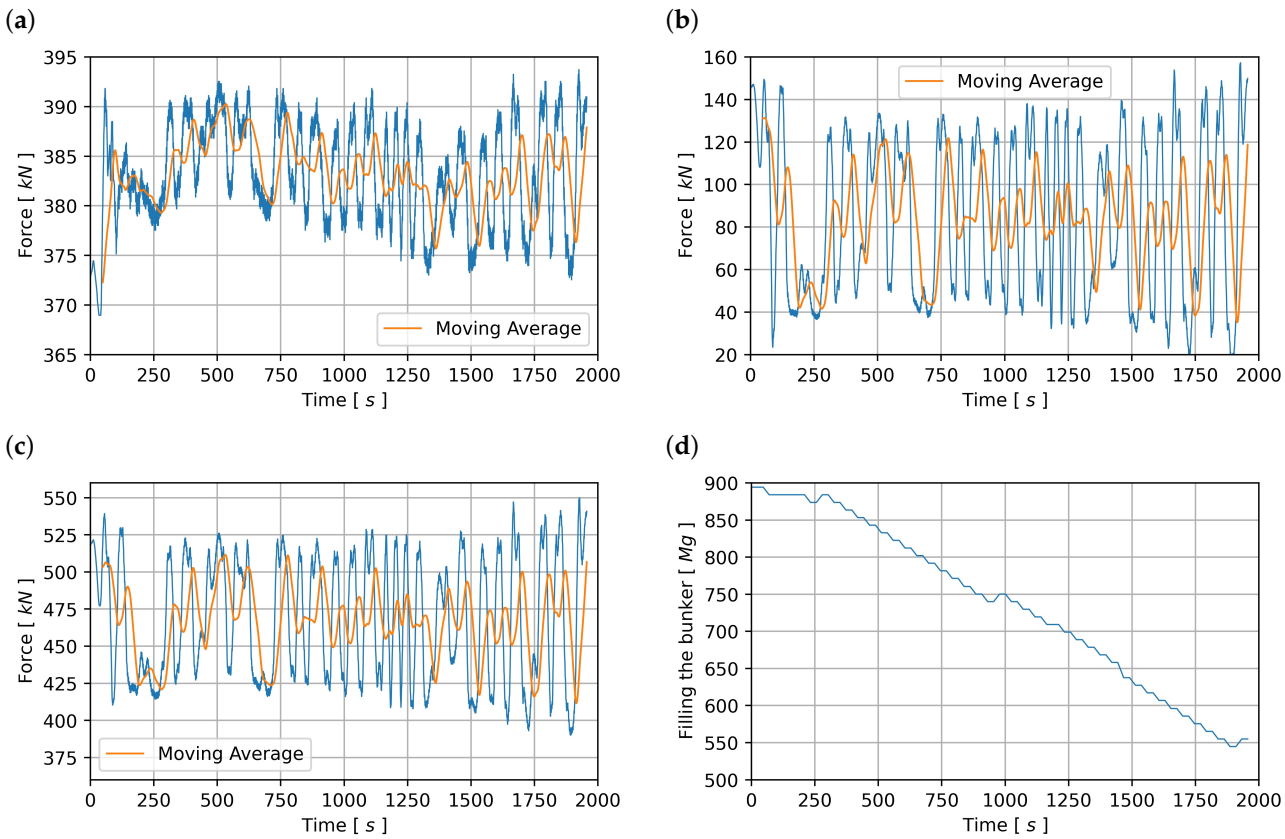


Figure 7. Calibration results of the DEM model on a real bin: (**a**) load on the front wheel supports, (**b**) load on the rear wheel supports, (**c**) cumulative load on all wheel supports, and (**d**) filling of the retention bunker during measurement.

4.2. DEM Model of the Current Bin

The filling of the bunker was realized through a virtual feeding point that generated the ore flow. This feeding point, located at the top of the retention bunker, simulated the operation of the actual feeding conveyor. It filled the retention bunker with ore at a rate

of 7200 Mg/h until a total mass of ore approx. 900 Mg was reached in the bunker. The simulation of emptying the retention bunker and the ore flow through the bin is shown in Figure 8. The simulation of the ore flow in the retention bunker revealed that in the initial phase, there is a core flow of ore, followed by the process of cascading ore from the subsequent layers forming a funnel. When the inclination of the funnel walls reaches an angle equal to the critical angle of respose, the final stage begins, during which the bin is emptied of the remaining ore. Only in this last phase is the ore located in the back part of the bin set in motion. The accumulation of material in the back part of the drawer is clearly visible in Figure 8. During normal operation of the bunkers, to protect the bin, complete emptying of the ore is prevented. Typically, a protective layer about 1 m thick is left above the upper plane of the bin crown. This is to protect the bin components from the falling ore from the feeding conveyor. Therefore, this operational inconvenience is common when using such devices. Calibration studies in real conditions also confirmed the uneven loading of the back part of the drawer. The predominant load concentrates in the front part of the drawer, which is located towards the outlet opening of the bin, as also demonstrated by measurements. The back part of the drawer is not proportionally loaded, causing most of the load to be transferred by the front wheel sets.

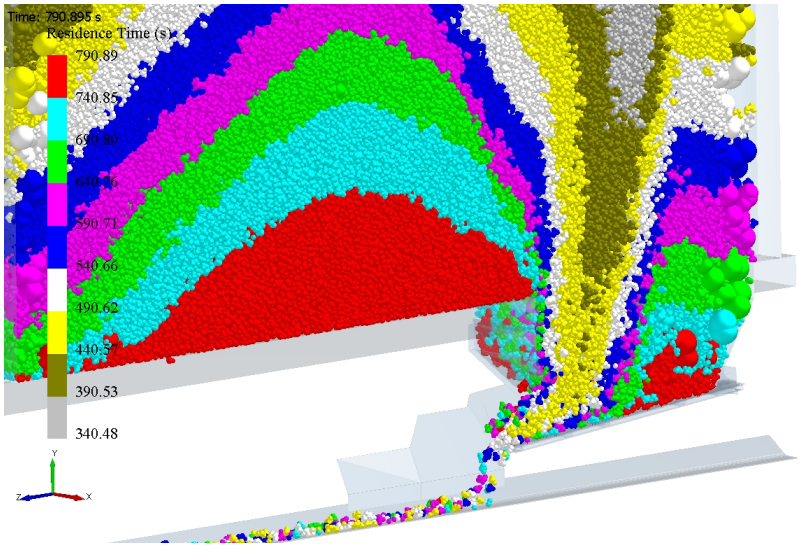


Figure 8. Ore flow in the current receiving bin in the EDEM environment.

Figure 9 presents the results of the bin operation simulation in the range of emptying the bunker from 900 Mg to 870 Mg (Figure 9b). This range was chosen based on operational experience, as it represents the most common working condition of the bin, and thus the entire analysis and optimization of the bin were conducted in this range. Figure 9a illustrates the changes in the pressure force from the vertical column of material on the bin drawer from the start until the bunker filling point reached 900 Mg. The pressure force on the drawer decreased from about 550 kN to 273 kN, where the load stabilized due to the organized flow of ore. Figure 9c shows how the capacity of the bin changed during the simulation. The average capacity was 588 Mg/h, fitting within the range of real values, which vary between 450 and 750 Mg/h depending on operational conditions. Figure 9d displays how the average particle velocity on the surface of the drawer changed, averaging 0.40 m/s. The fluctuations seen in the time signal are caused by the reciprocating motion of the drawer.

The differences between the pressures of ore on the receiving bin drawer measured in real working conditions and the values obtained in the simulation result from the simplification of the simulation model, particularly in the context of the digital ore model. Simplification of DEM model parameters can impact real results as this model does not account for all the complex physical and mechanical interactions occurring in the actual

environment. Nonetheless, the obtained load scale is close to the real values, which allows considering the simulation results as sufficient for further analysis and optimization. These studies aim to determine the direction of load changes, focusing less on their precise value.

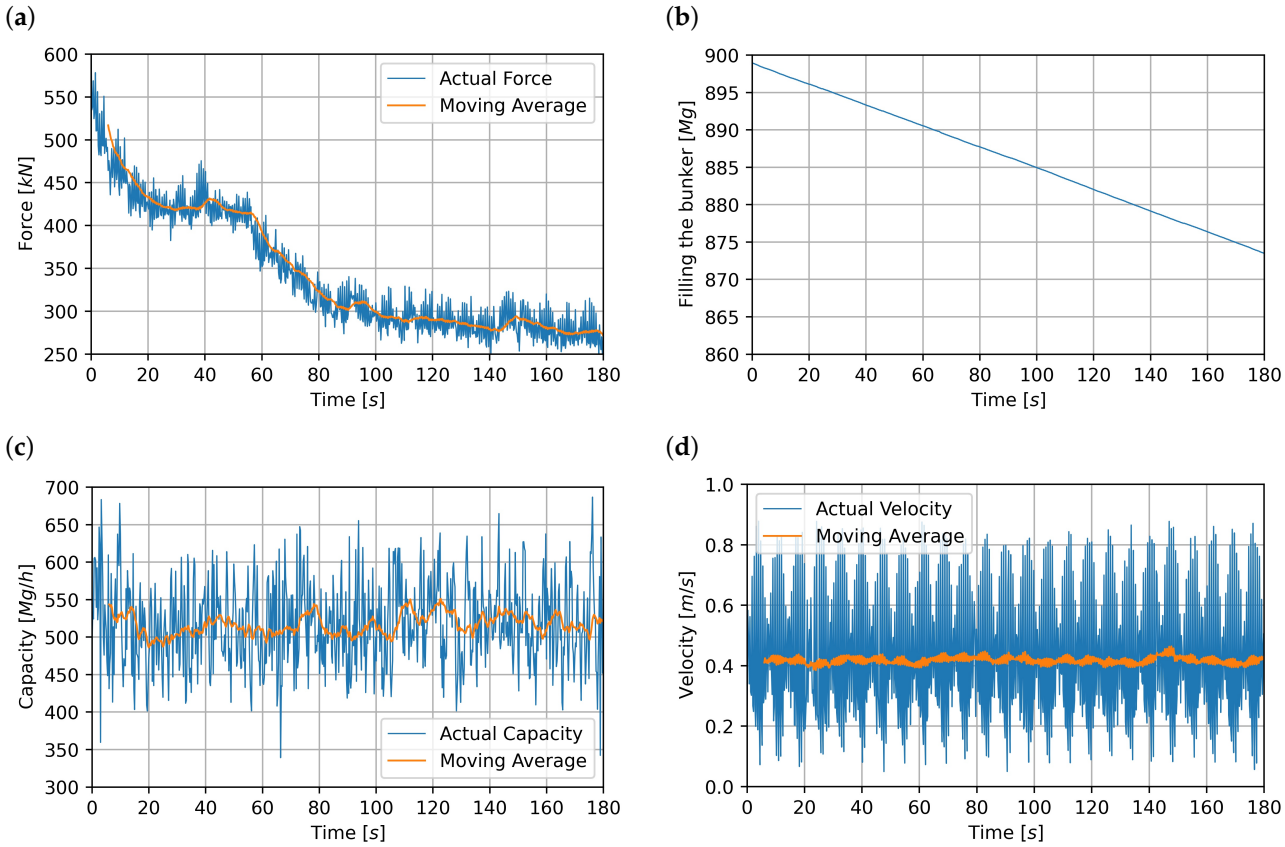


Figure 9. Parameters of the calibrated primary bin operation: (**a**) load on the bin drawer, (**b**) retention bunker filling, (**c**) bin capacity, and (**d**) average particle velocity on the bin drawer.

4.3. First Stage of Optimization

Figure 10 shows linear response surfaces as a function of independent factors for the first stage of the simulation. Table 4 presents the results of the Analysis of Variance (ANOVA) between each independent factor and the obtained responses.

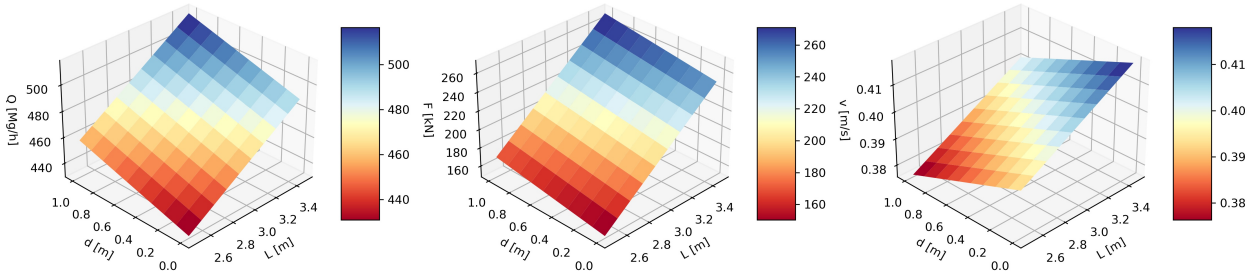


Figure 10. Response surfaces of the experiment for the first stage of the simulation.

Table 4. ANOVA test results (*p*-value) for the first stage of optimization.

Independent Factor	*F* [kN]	*v* [m/s]	*Q* [Mg/h]
L [m]	0.041	0.488	0.243
d [m]	0.887	0.605	0.695

Based on the obtained response surfaces and ANOVA results, it is clear that in this stage of the simulation, the length of the bin drawer L had the greatest impact on each of the dependent factors. A statistically significant impact of the bin length was observed only regarding the pressure force F on the drawer (p-value = 0.041). Given that the primary aim of the first stage was to reduce the pressure on the bin's drawer, the results are considered satisfactory as they correctly identified the influencing independent factor.

The offset of the bin from the axis of the bunker d had the most significant impact on capacity Q and particle velocity v, but this impact was considerably less pronounced than that of changing the length of the bin drawer L. No statistically significant effect was obtained for any case.

Based on the obtained response surfaces, a simplified optimization was carried out for the first stage of the simulation. In light of a 54% reduction in vertical force F on the drawer and only a slight decrease in capacity Q by 4%, the best variant was considered to be one where the length of the bin's drawer L was shortened by 1 m to 2.98 m, and the bin was offset d 1 m from the axis of the bunker compared to its current position. In this configuration, the vertical force F loading the drawer amounted to 155.5 kN, the average particle velocity v was reduced to 0.35 m/s, and the capacity Q remained practically unchanged, estimated at 484 Mg/h. The proposed design changes, based on the results of the first stage of the simulation, were introduced into the solid model of the bin and served as an entry point for the second stage of simulation.

4.4. Second Stage of Optimization

Figure 11 shows linear response surfaces as a function of independent factors for the second stage of the simulation. Table 5 presents the results of ANOVA test between each independent factor and the obtained responses.

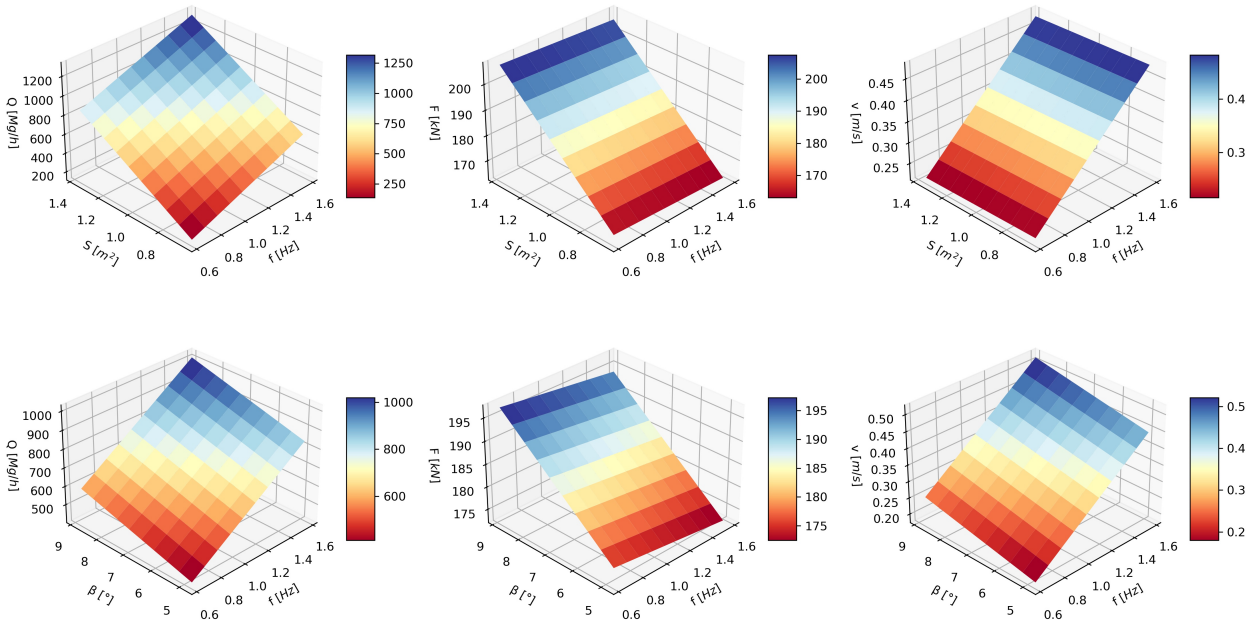


Figure 11. Response surfaces of the experiment for the second stage of the simulation.

Table 5. ANOVA test results (p-value) for the second stage of optimization.

Independent Factor	F [kN]	v [m/s]	Q [Mg/h]
f [Hz]	0.889	0	0.046
S [m^2]	0	0.892	0
β [°]	0.085	0.604	0.709

The results clearly show that the surface area of the outlet S and the inclination angle of the bin drawer β have the greatest impact on the vertical pressure force F on the drawer. However, a statistically significant effect was noted only for the surface area of the outlet S in relation to the force F. The frequency of the drawer movement f has virtually no effect on changes in the value of the pressure force F. Meanwhile, the most significant factor that statistically affects the average velocity v of particles on the surface of the bin drawer is the frequency of drawer movements f. The impact of the other two independent factors is much less, and additionally, their statistical significance is negligible. The capacity of the receiving bin Q is statistically determined only by the frequency of the drawer movements f and the surface area of the outlet S.

Figure 12 shows the results of the optimization algorithm in the form of the optimal operating point on the surfaces representing the relation of each dependent factor to the independent factor in the second stage of the simulation.

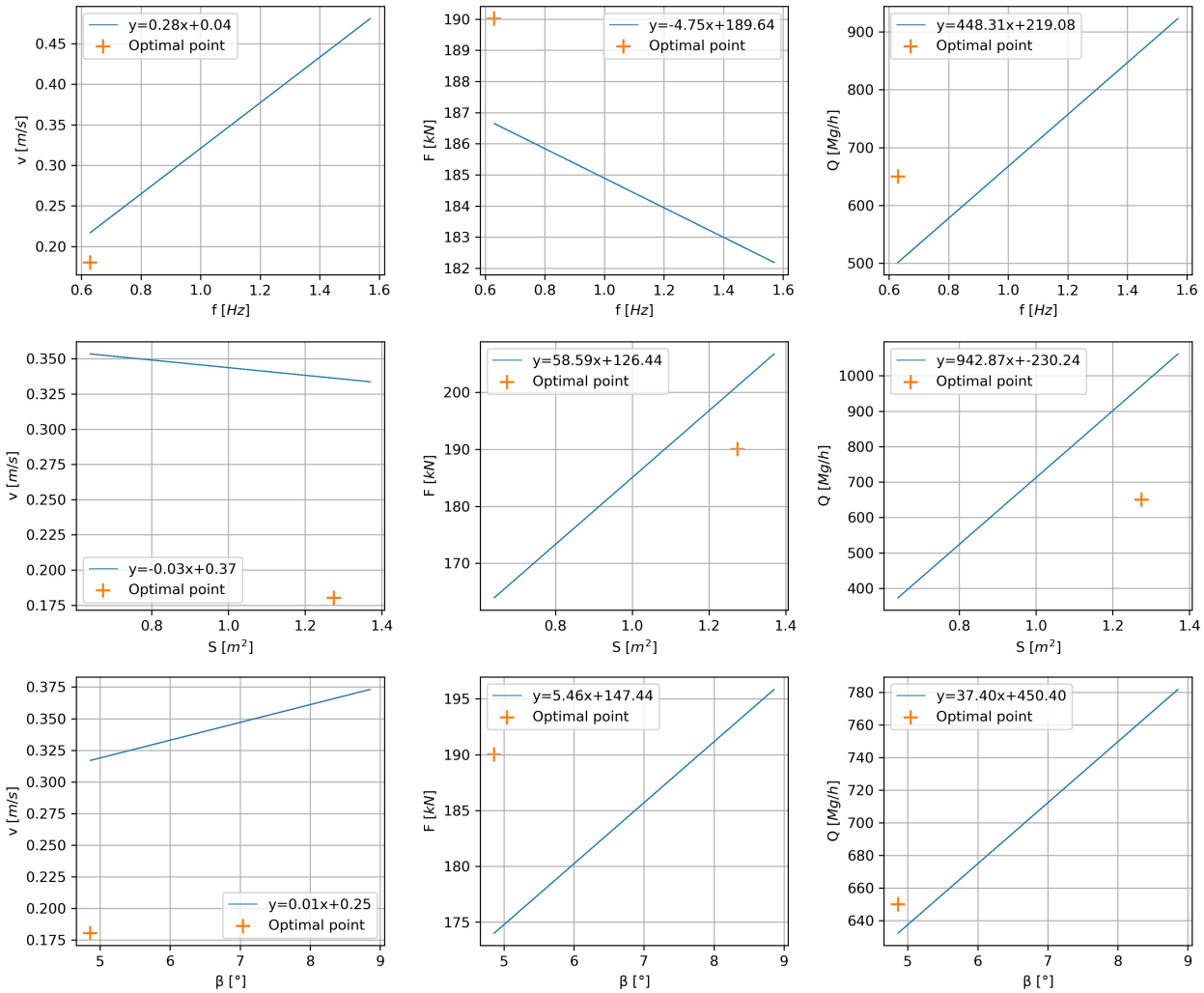


Figure 12. Optimization results using the gradient descent method with constraints—the optimal operating point determined for each response as a function of each independent factor.

The optimization algorithm results indicate that the most optimal operating point for the bin, considering the assumed constraints, is a configuration in which the bin operates at a frequency f of 0.63 Hz, with an outlet opening area S of 1.27 m², and a drawer inclination angle β of 4.86°. Under these conditions, the force F pressing on the drawer's surface is 190 kN, the average particle speed v is 0.19 m/s, and the capacity Q is maintained at about 650 Mg/h.

4.5. DEM Model of the Optimized Bin

A simulation was conducted for determined optimal point, similar to the original calibrated bin (Figure 8), to verify the expected force F, capacity Q, and particle velocity v on the drawer. Figure 13 illustrates the flow of ore in the optimized receiving bin, while Figure 14 shows the changes in all responses that were considered in the optimization process.

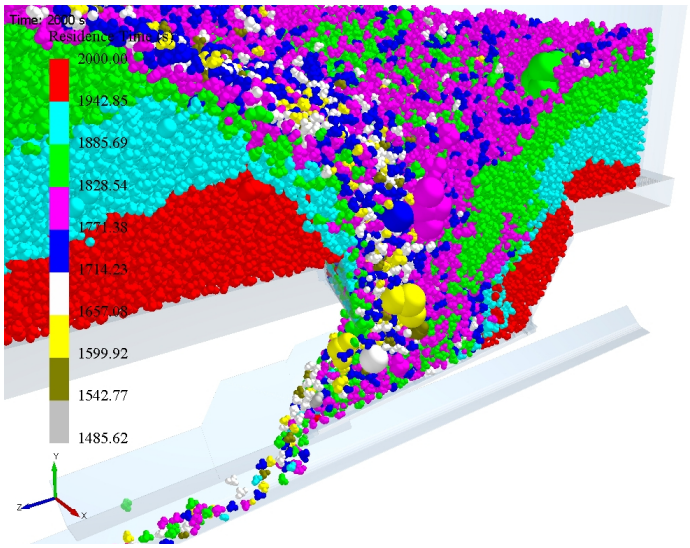


Figure 13. Ore flow in the optimized receiving bin in the EDEM environment.

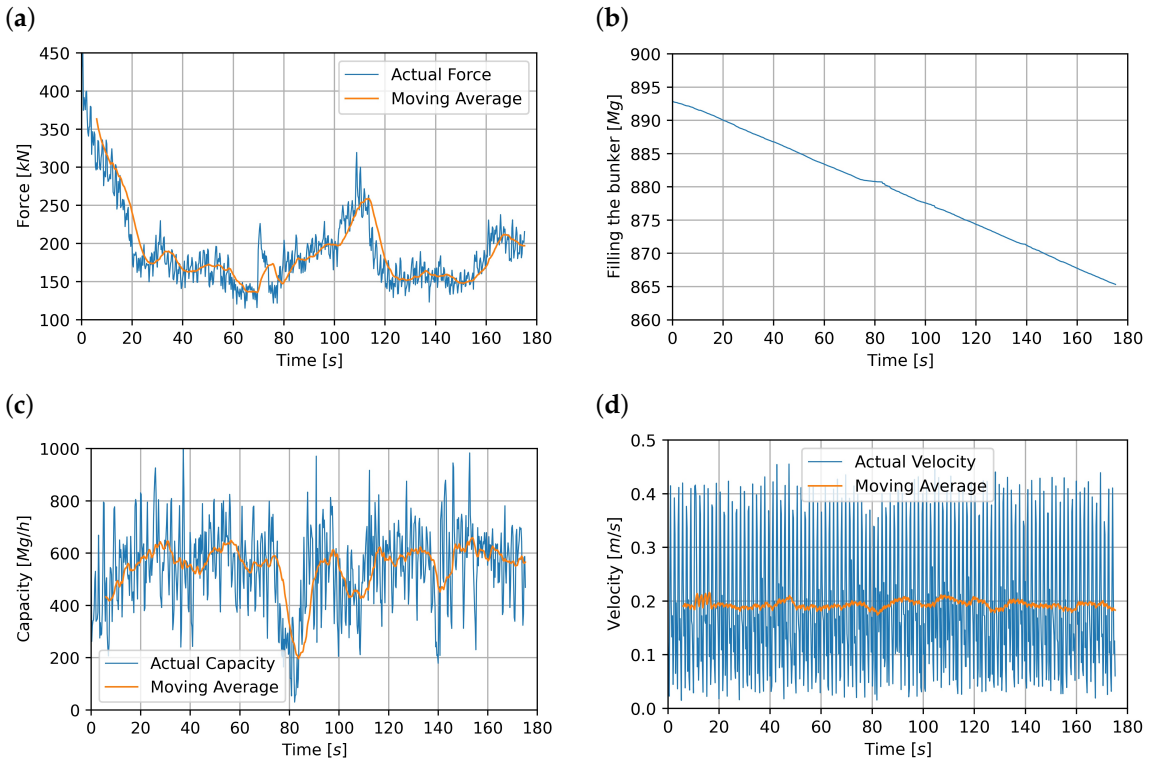


Figure 14. Parameters of the optimized bin operation: (**a**) load on the bin drawer, (**b**) retention bunker filling, (**c**) bin capacity, and (**d**) average particle velocity on the bin drawer.

5. Discussion

The observed discrepancy between the simulated and measured values, specifically the broader range of variation in simulated values (from 500 kN down to 275 kN) compared

to the relatively constant measured range (from 425 kN to 500 kN), can be attributed to several factors inherent in the DEM simulation. These may include model simplifications, assumptions regarding material properties, and the method used to represent the complex interactions and behaviors of copper ore particles within the bin. The constancy of measured values over a larger timescale and under conditions of significant decrease in the filling of the retention bunker suggests that the real-world system may exhibit buffering or compensatory mechanisms that are not fully captured or accurately represented in the simulation model. This could be due to the dynamic nature of ore flow and the feeder's response to varying load conditions, which may not be fully accounted for in the simulation parameters. To address this discrepancy and better match the measured values, we are considering several adjustments to the simulation parameters. These include refining the material properties of the copper ore (such as particle size distribution, shape, friction, and cohesion), improving the representation of the feeder and retention bunker geometry, and incorporating more dynamic feedback mechanisms that mimic the real-world system's response to changing conditions. Assuming that the simulation error is the same for all experiments, it is indeed possible to directly compare the results for the purpose of optimization, which has been accomplished in this article.

The analysis of data from various response surfaces allowed us to draw significant conclusions about the factors influencing the operation of the receiving bin. It was found that the two independent factors having the greatest impact on the force exerted on the bin's drawer F are the length of the drawer L and the surface area of the bin's outlet opening S. Another important aspect is the velocity of particles v on the surface of the drawer, which is primarily determined by the frequency of the drawer's movement f. This works in conjunction with the surface area of the bin's outlet opening S to collectively influence the capacity Q of the receiving bin. Among other independent factors, it was observed that the angle of inclination of the drawer β has some effect on the force exerted F, but its significance is not statistically important at the established level of confidence. Among all the factors analyzed, offset of the retention bunker axis d showed the least influence on the studied responses.

In Table 6, the primary and optimized values of the independent factors, as well as the responses obtained for them, are compiled.

Table 6. Comparison of primary and optimized values of independent factors.

Parameter	Unit	Primary Value	Optimized Value	Difference
L	m	3.98	2.98	−1
d	m	0	1	1
f	Hz	1.38	0.63	−0.75
S	m^2	0.72	1.27	0.55
β	°	4.86	4.86	0
F	kN	273	190	−83
Q	Mg/h	588	650	62
v	m/s	0.40	0.19	−0.21

The results obtained from the optimization algorithm are promising. To minimize the pressure force F on the drawer surface, it proved optimal to significantly reduce its length L and to maximize the offset of the receiving bin relative to the retention bunker's axis d. The achieved reduction in force F results from shortening the length of the receiving bin drawer L, which allowed for a reduction in its mass. Consequently, less material accumulates on the drawer, and the pressure exerted by the column of material is decreased, due to the concurrent shortening of the bin's feed chute from the retention bunker side. As a result, a smaller amount of material rests on the rear part of the drawer. The offset of the receiving bin relative to the retention bunker's axis d likely had a beneficial effect on altering the interactions between ore grains.

Efforts should also be made to use the lowest possible frequency of bin movement f and angle of inclination β to minimize the particle velocity v. If there is a need to increase capacity Q, the solution is to more than double the surface area of the outlet opening S. Simulations have shown that such changes can lead to a reduction in pressure force F by just over 30% and particle velocity v by more than 50%. Additionally, these changes have led to a slight increase in receptacle capacity Q by about 10%, resulting from improved ore flow through the receiving bin (increasing the S and decreasing f) and the elimination of material stagnation at the back of the bin drawer. A nearly 20% reduction in bin mass is also beneficial as it translates into reduced wear of structural elements and allows for extended trouble-free operation of the receiving bin and reduced maintenance work.

6. Conclusions

This article presents the results of optimizing the operation of an ore receiving bin in a retention bunker in an underground copper ore mine. The main factors causing excessive wear of the bin's drawer components are the pressure force from the vertical column of ore and the velocity of particles on the drawer's surface during its movement. A numerical experiment was proposed, which allowed for determining the relation between the basic construction and operational factors of the bins, and the pressure force on the drawer, the velocity of particles on the drawer's surface, and the capacity. To calibrate the ore flow model in the simulation environment, measurements of the drawer's load were conducted in real conditions of the underground copper ore mine. It was shown that the decisive factors affecting the pressure force of the ore on the drawer of the bin are its length and the surface area of the outlet opening. In the case of the particle velocity on the surface of the bin's drawer, the most significant impact on the obtained values was the frequency of the bin's movement.

The development of an optimized receiving bin design in a numerical simulation environment has enabled a significant reduction in pressure force and particle velocity, which will undoubtedly lead to a reduction in wear and tear during normal operational conditions. The next steps include the implementation of the optimized bin design into actual working conditions and the validation of the obtained results. The presented findings provide valuable knowledge that will influence the design of such devices in the future. Conducting a comparative analysis poses significant challenges due to the scarcity of literature on retention bunker constructions of similar scale. While there are descriptions of analogous or related structures, few studies address systems comparable in scale and specificity to those examined in our research. This rarity underscores the novelty of our study and contributes to the uniqueness of our methodology's application. Our solution undoubtedly offers improvements in operational costs for feeder systems. By reducing the frequency of drawer movements, our approach favorably impacts the electrical energy consumption of motors. Simultaneously, system efficiency is enhanced, potentially lowering the per-unit electrical energy consumption for each unit of material transported. Furthermore, the costs associated with the proposed modifications are minimal at the production stage, underscoring the practicality and cost-efficiency of our method. The full feasibility of our approach is demonstrated by the use of easily modifiable independent factors. This adaptability enhances the practical applicability of our optimization method, making it a viable option for real-world implementation.

During the optimization process, we focused on globally evaluated values for F and v. However, it is important to note that local correlations between these values and expected abrasive wear could lead to different optimization results. Regions with high particle velocity but low contact pressure might incur less wear than regions with high contact pressure and lower particle velocity. Therefore, a local coupling between force and velocity may be beneficial for future optimizations. This approach suggests that future research could benefit from more complex models that account for local interactions between operational parameters and abrasive wear. The development and application of such models could enable more precise adjustments to operational processes to minimize

wear and extend the lifespan of equipment. This opens new avenues for research in the optimization of flow systems, emphasizing the importance of understanding local effects within the context of global optimization strategies.

Author Contributions: P.B.: conceptualization, methodology, software, validation, formal analysis, investigation, data curation, writing—original draft preparation, visualization; R.K.: conceptualization, methodology, formal analysis, investigation, writing—review and editing, supervision, project administration, funding acquisition; N.S.-M.: conceptualization, methodology, validation, formal analysis, investigation, writing—original draft preparation; M.O.: conceptualization, methodology, validation, formal analysis, investigation, writing—original draft preparation; M.S.: conceptualization, methodology, software, validation, formal analysis, investigation, resources, data curation, writing—review and editing, visualization. All authors have read and agreed to the published version of the manuscript.

Funding: The research work was funded with the research subsidy from the Polish Ministry of Science and Higher Education granted for 2024.

Institutional Review Board Statement: Not applicable.

Informed Consent Statement: Not applicable.

Data Availability Statement: The data are available upon email contact with the corresponding author. The data are not publicly available due to privacy.

Acknowledgments: The results presented in this article were part of research conducted in connection with the doctoral implementation work carried out in cooperation with KGHM Polska Miedź S.A. We would like to express our sincere gratitude for their assistance in conducting the research, as well as for their technical and substantive support.

Conflicts of Interest: Author Mateusz Szczerbakowicz was employed by the company KGHM Polska Miedź S.A. The remaining authors declare that the research was conducted in the absence of any commercial or financial relationships that could be construed as a potential conflict of interest.

References

1. Saderova, J.; Rosova, A.; Kacmary, P.; Sofranko, M.; Bindzar, P.; Malkus, T. Modelling as a Tool for the Planning of the Transport System Performance in the Conditions of a Raw Material Mining. *Sustainability* **2020**, *12*, 8051. [CrossRef]
2. Bardzinski, P.; Jurdziak, L.; Kawalec, W.; Krol, R. Copper ore quality tracking in a belt conveyor system using simulation tools. *Nat. Resour. Res.* **2020**, *29*, 1031–1040. [CrossRef]
3. Gavrishev, S.; Burmistrov, K.; Tomilina, N. Increasing the work scope of conveyor transport at mining companies. *Procedia Eng.* **2016**, *150*, 1317–1321. [CrossRef]
4. Scott, O.; Choules, P. The use of impact plates in conveyor transfers. *Tribol. Int.* **1993**, *26*, 353–359. [CrossRef]
5. Szczerbakowicz, M.; Suchorab, N.; Król, R. Preliminary Failure Frequency Analysis of Receiving Bins in Retention Bunkers Operated in Underground Copper Ore Mines. *Appl. Sci.* **2021**, *11*, 3628. [CrossRef]
6. Gutierrez, A.; Garate, G. Design of a transfer chute for multiple operating conditions. In Proceedings of the ASME International Mechanical Engineering Congress and Exposition, Montreal, QC, Canada, 14–20 November 2014; American Society of Mechanical Engineers: New York, NY, USA, 2014; Volume 46606, p. V011T14A005.
7. Roberts, A.W. Chute performance and design for rapid flow conditions. *Chem. Eng. Technol. Ind. Chem.-Plant Equip.-Process Eng.-Biotechnol.* **2003**, *26*, 163–170. [CrossRef]
8. Walker, P.; Kawalec, W.; Król, R. Application of the discrete element method (DEM) for simulation of the ore flow inside the shaft ore bunker in the underground copper ore mine. In Proceedings of the Intelligent Systems in Production Engineering and Maintenance, Wrocław, Poland, 13–15 September 2018; Springer: Cham, Switzerland, 2019; pp. 633–644.
9. Molnár, V.; Fedorko, G.; Husáková, N.; Král', J., Jr.; Ferdynus, M. Energy calculation model of an outgoing conveyor with application of a transfer chute with the damping plate. *Mech. Sci.* **2016**, *7*, 167–177. [CrossRef]
10. Ilic, D.; Katterfeld, A. Simulation of Transfer Chutes. *Simulations in Bulk Solids Handling: Applications of DEM and Other Methods*; Wiley: Hoboken, NJ, USA, 2023; pp. 41–78.
11. Basu, S.; Chakrabarty, A.; Nag, S.; Chaudhary, P.; Sinha, S.; Jain, T.; Nainegali, M.S.; Rodriguez, V.A.; Tavares, L.M. Modeling and simulation of mechanical degradation of iron ore sinter in a complex transfer chute system using the discrete element model and a particle breakage model. *Powder Technol.* **2023**, *417*, 118264. [CrossRef]
12. Esmaieli, K.; Hadjigeorgiou, J. Selecting ore pass-finger raise configurations in underground mines. *Rock Mech. Rock Eng.* **2011**, *44*, 291–303. [CrossRef]

13. Gopaul, K.; Venkannah, S.; Dauhoo, M.Z. Wear and flow rate problems on chutes in a rock crushing plant. *Tribol. Mater.* **2022**, *1*, 128–137. [CrossRef]
14. Jeyaprakash, N.; Yang, C.-H. Friction, lubrication, and wear. In *Tribology in Materials and Manufacturing-Wear, Friction and Lubrication*; IntechOpen: London, UK, 2020; pp. 1–7.
15. Çeçen, F.; Aktaş, B.; Özbayrak, A. Non-destructive triaxial vibroacoustic modal testing with a single sound transducer: A railway sleeper case study. In *Nondestructive Testing and Evaluation*; Taylor & Francis: Abingdon, UK, 2023; pp. 1–20.
16. WAlker, P.; Doroszuk, B.; Król, R. Analysis of ore flow through longitudinal belt conveyor transfer point. *Eksploat. Niezawodn.* **2020**, *22*.
17. Karwat, B.; Rubacha, P.; Stańczyk, E. Simulational and experimental determination of the exploitation parameters of a screw conveyor. *Eksploat. Niezawodn.* **2020**, *22*, 741–747. [CrossRef]
18. Kukreja, K.; Soni, M.K.; Nainegali, M.S.; Mohapatra, B. Development of transfer chute design through Discrete Element Modelling for using Refused Derived fuel in Indian cement plants. *Sustain. Energy Technol. Assessments* **2022**, *53*, 102567. [CrossRef]
19. Xia, R.; Wang, X.; Li, B.; Wei, X.; Yang, Z. Discrete element method-(DEM-) based study on the wear mechanism and wear regularity in scraper conveyor chutes. *Math. Probl. Eng.* **2019**, *2019*, 4191570. [CrossRef]
20. Xu, Y.; Zhang, C.; Zhao, J.; Li, W.; Qin, Y.; Lin, J. Optimization Design and Application of Material Transfer Device Based on DEM. In Proceedings of the IEEE 2019 International Conference on Advances in Construction Machinery and Vehicle Engineering (ICACMVE), Changsha, China, 14–16 May 2019; pp. 29–33.
21. Gan, J.; Evans, T.; Yu, A. Application of GPU-DEM simulation on large-scale granular handling and processing in ironmaking related industries. *Powder Technol.* **2020**, *361*, 258–273. [CrossRef]
22. Ilic, D.; Roberts, A.; Wheeler, C.; Katterfeld, A. Modelling bulk solid flow interactions in transfer chutes: Shearing flow. *Powder Technol.* **2019**, *354*, 30–44. [CrossRef]
23. Ilic, D.; Lavrinec, A.; Orozovic, O. Simulation and analysis of blending in a conveyor transfer system. *Miner. Eng.* **2020**, *157*, 106575. [CrossRef]
24. Xie, L.; Zhong, W.; Zhang, H.; Yu, A.; Qian, Y.; Situ, Y. Wear process during granular flow transportation in conveyor transfer. *Powder Technol.* **2016**, *288*, 65–75. [CrossRef]
25. Ye, F.; Qiang, Y.; Jiang, W.; Fu, X. DEM–FEM Coupling Simulation of the Transfer Chute Wear with the Dynamic Calibration DEM Parameters. *Processes* **2021**, *9*, 1847. [CrossRef]
26. Ilic, D. Development of design criteria for reducing wear in iron ore transfer chutes. *Wear* **2019**, *434*, 202986. [CrossRef]
27. Nematollahi, E.; Zare, S.; Maleki-Moghaddam, M.; Ghasemi, A.; Ghorbani, F.; Banisi, S. DEM-based design of feed chute to improve performance of cone crushers. *Miner. Eng.* **2021**, *168*, 106927. [CrossRef]
28. Li, X.; Jiang, Q.; Long, Y.; Chen, Z.; Zhao, W.; Ming, W.; Cao, Y.; Ma, J. Design Optimization of Chute Structure Based on E-SVR Surrogate Model. *Metals* **2023**, *13*, 635. [CrossRef]
29. Xia, R.; Wang, X.; Li, B.; Wei, X.; Yang, Z. The prediction of wear on a scraper conveyor chute affected by different factors based on the discrete element method. *Proc. Inst. Mech. Eng. Part C J. Mech. Eng. Sci.* **2019**, *233*, 6229–6239. [CrossRef]
30. Xia, R.; Li, B.; Wang, X.; Yang, Z.; Liu, L. Screening the Main Factors Affecting the Wear of the Scraper Conveyor Chute Using the Plackett–Burman Method. *Math. Probl. Eng.* **2019**, *2019*, 1204091. [CrossRef]
31. Ma, H.; Wang, X.; Li, B.; Liu, Z.; Bi, W.; Wei, X. Study on the mechanical effect and wear behaviour of middle trough of a scraper conveyor based on DEM–MBD. *Proc. Inst. Mech. Eng. Part J J. Eng. Tribol.* **2022**, *236*, 1363–1374. [CrossRef]
32. Haji, S.H.; Abdulazeez, A.M. Comparison of optimization techniques based on gradient descent algorithm: A review. *PalArch's J. Archaeol. Egypt/Egyptol.* **2021**, *18*, 2715–2743.
33. Chen, G.; Li, Q.; Li, D.; Wu, Z.; Liu, Y. Main frequency band of blast vibration signal based on wavelet packet transform. *Appl. Math. Model.* **2019**, *74*, 569–585. [CrossRef]
34. Chen, G.; Yang, J.; Liu, Y.; Kitahara, T.; Beer, M. An energy-frequency parameter for earthquake ground motion intensity measure. *Earthq. Eng. Struct. Dyn.* **2023**, *52*, 271–284. [CrossRef]
35. Hertz, H. The contact of elastic solids. *J. Reine Angew. Math.* **1881**, *92*, 156–171.
36. Di Renzo, A.; Di Maio, F.P. Comparison of contact-force models for the simulation of collisions in DEM-based granular flow codes. *Chem. Eng. Sci.* **2004**, *59*, 525–541. [CrossRef]
37. Mindlin, R.D. Compliance of elastic bodies in contact. *J. Appl. Mech.* **1949**, *16*, 259–268. [CrossRef]
38. Mindlin, R.D.; Deresiewicz, H. Elastic spheres in contact under varying oblique forces. *J. Appl. Mech.* **1953**, *20*, 327–344. [CrossRef]
39. Gelnar, D.; Zegzulka, J. Discrete Element Method in the Design of Transport Systems. In *Verification and Validations of 3D Models*; Springer: Cham, Switzerland, 2019; pp. 5–15.
40. Ozdoba, M.; Krol, R. Grain Size Distribution of Copper Ore as Means for Qualitative Evaluation of Its Lithological Composition. *IOP Conf. Ser. Earth Environ. Sci.* **2019**, *221*, 012100. [CrossRef]
41. Doroszuk, B.; Walker, P.; Król, R. Investigation of properties of lithologically diversified copper ore for DEM modeling. *CUPRUM-Nauk.-Tech. Górnictwa Rud* **2019**, *90*, 5–19.

Disclaimer/Publisher's Note: The statements, opinions and data contained in all publications are solely those of the individual author(s) and contributor(s) and not of MDPI and/or the editor(s). MDPI and/or the editor(s) disclaim responsibility for any injury to people or property resulting from any ideas, methods, instructions or products referred to in the content.